Materials Transactions, Vol. 47, No. 4 (2006) pp. 1121 to 1126

Categorization of Ambient-Temperature Creep Behavior of Metals and Alloys on Their Crystallographic Structures*[1]

Eiichi Sato[1,*2], Tomoyasu Yamada[1,*3], Hisamune Tanaka[1,*4] and Itaru Jimbo[2]

[1]*Institute of Space and Astronautical Science, Japan Aerospace Exploration Agency (ISAS/JAXA), Sagamihara 229-8510, Japan*
[2]*School of Engineering, Tokai University, Hiratsuka 259-1292, Japan*

The creep behavior at an ambient temperature of typical h.c.p., b.c.c. and f.c.c. metals and alloys of annealed states were surveyed. Cubic metals and alloys demonstrated negligible creep strain under all stress ranges. In contrast, h.c.p. metals and alloys demonstrated significant creep behavior. In particular, Ti–6Al–4V alloy and CP–Ti metal showed accumulated large creep strains. The difference among metals and alloys were negligible, for Mg and Zr. After being cold rolled, Ti–6Al–4V alloy and CP–Ti metal showed less significant creep behavior.

(Received October 3, 2005; Accepted January 6, 2006; Published April 15, 2006)

Keywords: *creep, titanium alloy, h.c.p. metals and alloys, primary creep*

1. Introduction

Titanium alloys are attractive materials for structural applications in aerospace systems because of their high strength to weight ratio, high corrosion resistance and ability of superplastic blow forming. The fuel tank of the electric propulsion system of HAYABUSA, the ISAS/JAXA satellite for the asteroid sample return mission launched in May 2003, is made of Ti–6Al–4V alloy. During the proof test of the tank, creep phenomenon was observed at an ambient temperature and under stresses below the yield stress. Although small amount of creep strain in a fuel tank might be permissible, creep in fasteners, *i.e.* bolts and nuts, cannot be permitted since it would cause stress relaxation that could lead to a very dangerous state.

The presence of significant creep at an ambient temperature in titanium alloys was reported in Ti–5Al–2.5Sn alloy[1)] and Ti–6Al–4V alloy[2,3)] in the 1960s. However, the study did not continue except those of Ti–6Al–2Cb–1Ta–1Mo alloy[4)] and Ti–0.4Mn alloy[5)] at around 1990. In the 1990s, the group of Mills started studying the phenomena using Ti–6Al–2Sn–4Zr–2Mo alloy[6,7)] and Ti–6Al alloy.[7–9)]

It was suggested[2)] that the mechanism of the ambient-temperature creep is due to Andrade creep.[10)] Also it was suggested that twining is relating to the phenomena.[5)] Recently, it was claimed that the straight array of dislocations, which was formed by solute Al atoms, had an important roll to the creep.[7,8)] However those are suppositions based only on the individual experiments unique for the tested materials. Especially, we need a critical discussion whether Ti–Al solid solution system is necessary for the creep.

In the present study, aiming at the understanding of this ambient-temperature creep mechanism of titanium alloys as the final purpose, we performed a surveying study of ambient-temperature creep in several metals and alloys having various crystallographic structures. First, we focused on titanium alloys, and performed creep tests using α-Ti, $(\alpha+\beta)$-Ti and β-Ti. Then we compared the creep behavior of other metals and alloys of different crystallographic structures. The creep behavior, some of which has been already reported,[11)] was analyzed quantitatively using the logarithmic creep equation.

2. Experimental

As described in § Introduction, we performed a surveying study of ambient-temperature creep in several metals and alloys of h.c.p., b.c.c. and f.c.c. structures; h.c.p. materials were classified by c/a ratio and the primary slip system. The material such as Zn to whom the ambient temperature is higher than 0.4 of the melting point in Kelvin, was not used. Table 1 lists the abbreviation, chemical composition and heat treatment of the materials studied. All the materials except pure Mg and AZ31, which were hot-rolled at 573 K, and pure Fe, which was cold-rolled, were in annealed condition. Cold-rolled CP–Ti of 55% reduction and cold-rolled Ti–64 of 40% reduction were also examined. Though Ti-64 had $(\alpha+\beta)$ dual-phase structure, it was categorized into h.c.p. materials since h.c.p. phase seemed to dominate the creep behavior.

The tensile and creep specimens were cut using electro-spark machining, and the heat affected zone was polished by emery paper of #800. Tensile tests were performed using an Instron-type machine under a constant nominal strain rate of $1\times10^{-2}\,s^{-1}$ to determine 0.2% proof strength ($\sigma_{0.2}$). The stress axes of the specimens were parallel to the extrusion or rolling axes.

Creep tests were performed at an ambient temperature under a constant load condition for 24 h with stress axes parallel to the extrusion or rolling axes. The applied stresses were set on the basis of the measured $\sigma_{0.2}$ for each material. Special creep specimens having four cross sections with different areas were machined, as shown in Fig. 1. The strain was measured using strain gauges of resolution $\pm3\times10^{-6}$ mounted directly on the surface of the four positions of the specimens.

In this study we had to consider the creep of a strain gage itself, which is the phenomenon that an inverse strain is

*[1]This Paper was Originally Published in Japanese in J. JILM **55** (2005) 604.
*[2]Corresponding author, E-mail: sato@isas.jaxa.jp
*[3]Graduate Student, Tokai University (Present address: Sankyo Aluminium Industry co. ltd.)
*[4]Graduate Student, Tokai University

Table 1 Chemical composition, heat treatment and measured 0.2% proof stress of the tested metals and alloys.

Specimen	Chemical Composition (wt%)	Heat Treatment	0.2% Proof Stress
CP–Ti	Ti–0.25Fe–0.2O–0.015H–0.08C–0.03N	973 K, AC	252 MPa
CP–Ti(CR)	Ti–0.25Fe–0.2O–0.015H–0.08C–0.03N	973 K, AC + CR 55%	592 MPa
Ti-64	Ti–6Al–4V–0.4Fe–0.2O–0.08C–0.05N–0.015H	978 K, AC	981 MPa
Ti-64(CR)	Ti–6Al–4V–0.4Fe–0.2O–0.08C–0.05N –0.015H	978 K, AC + CR 40%	1018 MPa
Ti-15333	Ti–15V–3Al–3Cr–3Sn–0.25P–0.05N–0.05C–0.13O–0.1H	1073 K, AC	765 MPa
Pure Zr	99.2Zr	1123 K, AC	194 MPa
Zircaloy	Zr–1.56Sn–0.11Cr–0.22Fe–0.12O	950 K, AC	380 MPa
Pure Mg	99.95 Mg	573 K, HR	67 MPa
AZ31	Mg–3Al–1Zn–0.03Mn–0.01Fe–0.005Ni–0.005Cu–0.02Si	573 K, HR	193 MPa
Pure Fe	99.99Fe	CR	363 MPa
1050Al	99.5Al	623 K, AC	96 MPa
5052Al	Al–2.5Mg–0.4Fe–0.25Cr–0.25Si– 0.1Cu–0.1Mn–0.1Zn	523 K, AC	197 MPa

AC: air cooling, CR: cold roll, HR: hot roll

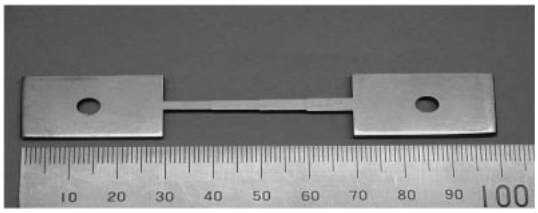

Fig. 1 Creep specimen with four cross sections.

outputted against the load with time when a large strain is applied on a gage attached on a specimen. It occurs mainly because of the creep of the adhesive attaching the gage on the specimen. Thorough both using the gage with long turn-tubs (the part where the resistance line is turned back) and applying a proper recommended adhesion procedure, the specimen strain was transferred to the resistance line correctly and thus we could reduce the phenomenon of gage creep. Under the condition of the maximum stress in Ti-15333, we measured a positive strain rate of $3 \times 10^{-10}\,s^{-1}$ ($\dot{\varepsilon}_s$, defined later, was much smaller than that). Therefore we could estimate that the accuracy of the strain rate measurement was about this order.

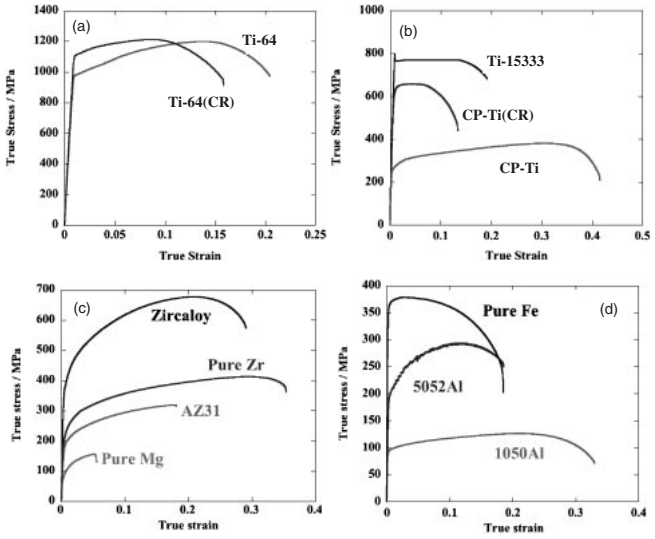

Fig. 3 True stress-true strain curves of (a) Ti-64 and Ti-64(CR), (b) CP–Ti, CP–Ti(CR) and Ti-15333, (c) pure Mg, AZ31, pure Zr and Zircaloy, and (d) 1050Al, 5052Al and pure Fe.

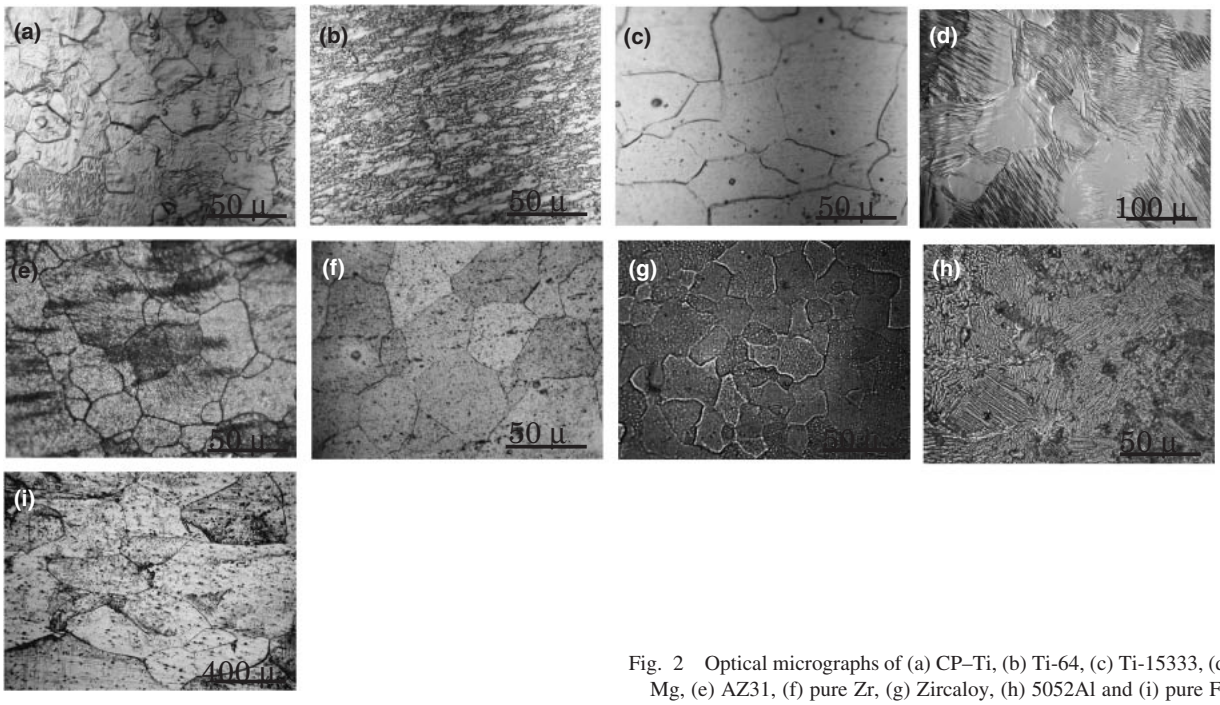

Fig. 2 Optical micrographs of (a) CP–Ti, (b) Ti-64, (c) Ti-15333, (d) pure Mg, (e) AZ31, (f) pure Zr, (g) Zircaloy, (h) 5052Al and (i) pure Fe.

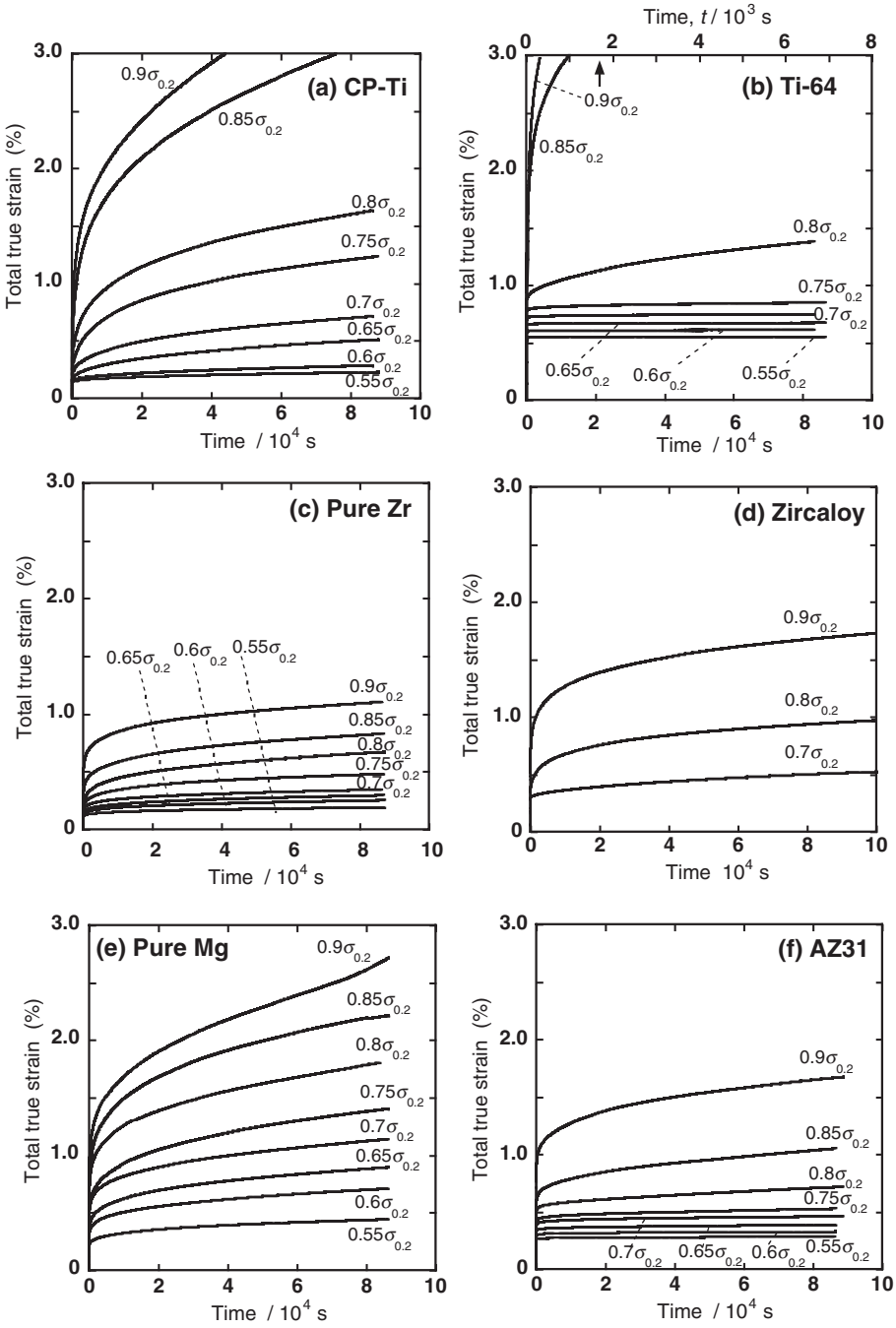

Fig. 4 Creep curves of hexagonal metals and alloys.

3. Results

3.1 Microstructural observation

Figure 2 shows some examples of optical microscopy. CP–Ti, Ti-15333, pure Mg, AZ31, pure Zr, zircaloy, 5052Al and pure Fe had almost equiaxed grains and their average grain size, determined by the mean linear intercept method, were 20, 40, 120, 27, 36, 21, 32, 450 μm, respectively. Ti-64 had elongated grains of 10×20 μm oriented in the extrusion direction.

3.2 Stress–strain curves

Figure 3 shows the true stress-true strain curves obtained in the tensile tests with the initial strain rate of $1 \times 10^{-2}\,s^{-1}$. Ti-64 and Ti-15333 show upper and lower yield points. Other metals and alloys show smooth yielding behavior, and only 5052Al shows serration behavior. The cold-rolled CP–Ti and Ti-64 show higher $\sigma_{0.2}$ and lower fracture strain than the corresponding annealed ones, but similar yielding behavior with those. The value of $\sigma_{0.2}$ of each material, given in Table 1, was obtained from the average of three tests.

3.3 Creep curves

Figure 4 are creep curves of h.c.p. metals and alloys, showing significant creep at an ambient temperature both in the primary region and in the steady-state region. Among h.c.p. materials, Ti metal and alloy show more extended creep than other materials such as Mg and Zr. For example,

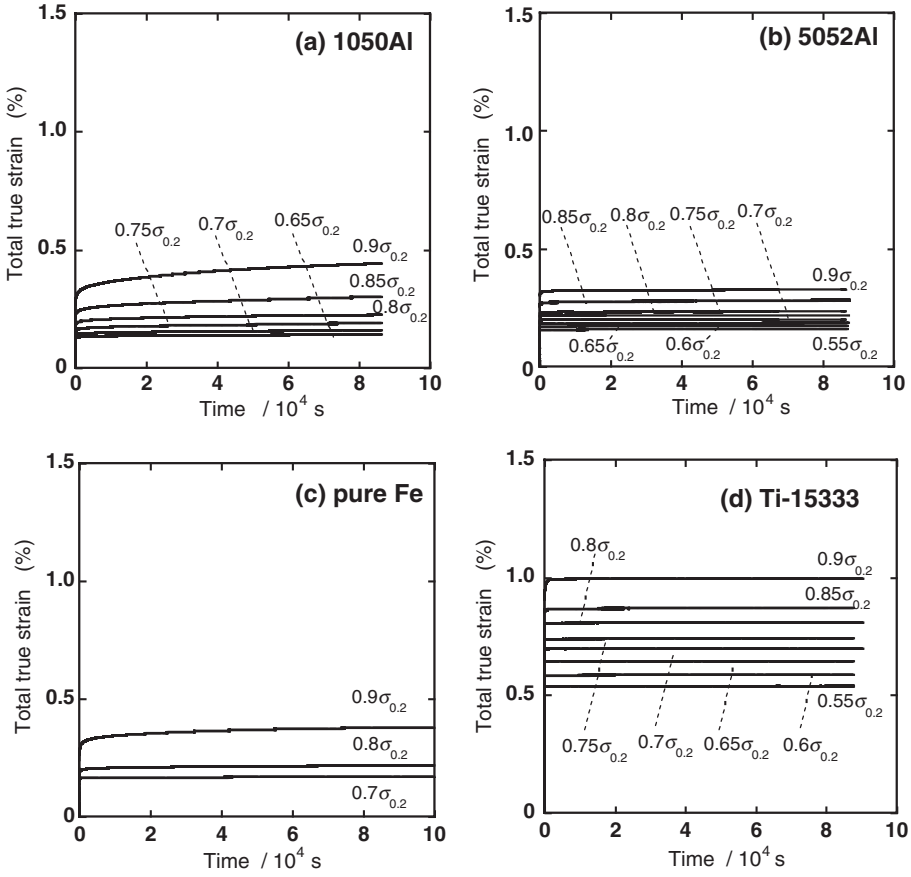

Fig. 5 Creep curves of cubic metals and alloys.

Ti-64 and CP–Ti showed significant creep behavior and accumulated large creep strain of more than 1% in 90 and 1600 s, respectively under $0.9\sigma_{0.2}$.

Figure 5 shows creep curves of b.c.c. and f.c.c. metals and alloys. Similarly to h.c.p. materials, f.c.c. and b.c.c. metals demonstrated primary creep, but the accumulated creep strain was much smaller; even 1050Al accumulated only 0.1% during 8000 s under $0.9\sigma_{0.2}$. It should be noted that the range of vertical axes of Figs. 4 and 5 are different. Further on, f.c.c. and b.c.c. alloys demonstrated negligible creep under the accuracy of the experiments.

4. Discussion

4.1 Quantitative analysis of creep behavior

Each measured creep curve was, then, fitted by the logarithmic creep equation, eq. (1),

$$\varepsilon = \varepsilon_{\mathrm{i}} + \varepsilon_0 \ln(1 + \beta_0 t) + \dot{\varepsilon}_{\mathrm{s}} t, \tag{1}$$

where ε is the total strain, ε_{i} is the instantaneous strain on loading, ε_0 and β_0 are the coefficients of primary creep, t is the testing time and $\dot{\varepsilon}_{\mathrm{s}}$ is the extrapolated minimum creep rate. Figure 6 shows creep curves of CP–Ti under $0.8\sigma_{0.2}$ as an example of the fitting. It is obvious that the fitted curve reproduces the experimental point (○) quite well. The fitting was performed on the all creep curves except those of $\dot{\varepsilon}_0 < 10^{-10}\,\mathrm{s}^{-1}$; they were estimated as $\dot{\varepsilon}_0 = 0\,\mathrm{s}^{-1}$.

Figure 7 shows the double-logarithmic plot of the minimum creep rate and the applied stress normalized by Young's modulus. We can categorize the data plots into three groups based on the crystallographic structure and alloying of the materials. The group of low stress and high strain rate is for pure metals of h.c.p., that of high stress and high strain rate is for solid solution alloys of h.c.p., and that of low stress, which is almost out of the figure range, is for cubic metals and alloys.

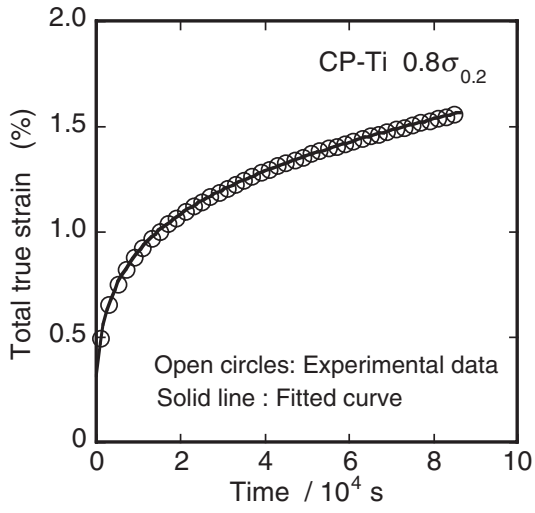

Fig. 6 Example of creep curve fitting of CP–Ti under $0.8\sigma_{0.2}$ by the logarithmic creep equation. The experimental data are shown by circles and the fitted result is shown by a solid line.

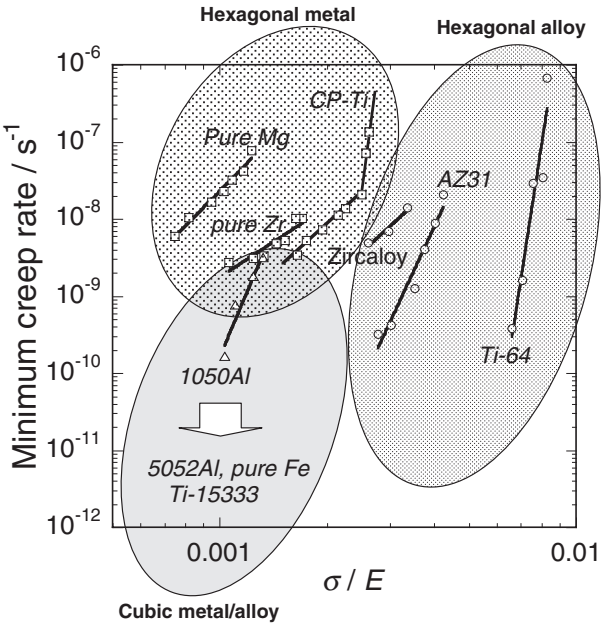

Fig. 7 Double logarithmic plot of the minimum creep rate and the stress normalized by Young's modulus. The minimum creep rates were obtained through fitting of the logarithmic creep equation on the creep data of 8×10^4 s' duration.

Almost all of the materials show straight dependency in a double-logarithmic plot of the minimum creep rate and applied stress, and expressed by the following power-law creep equation,

$$\dot{\varepsilon}_s = \dot{\varepsilon}_{s0.2}\left(\frac{\sigma}{\sigma_{0.2}}\right)^n, \tag{2}$$

where n is the stress exponent and $\dot{\varepsilon}_{s0.2}$ is the assumed minimum creep rate under the applied stress of $\sigma_{0.2}$.

Metals of h.c.p. show the stress exponent from 3 to 5 except the highest stress region of CP–Ti, where the behavior similar to the power-law creep break down is observed. In addition, the data of CP–Ti locate in the highest stress region among the tree, since the elastic limit strain of Ti is the highest and thus the data region based on the $\sigma_{0.2}$ also locates in the highest region.

Mg has an ideal c/a ratio of 1.62, while Ti and Zr have smaller c/a ratio of 1.59. Therefore the primary slip system of Ti and Zr is expected to be prismatic, while that of Mg is basal. The observed ambient-temperature creep behavior dose not reflect the expected variation in the slip system.

The data of h.c.p. alloys locate in the higher stress region than those of h.c.p. metals because of an increase in $\sigma_{0.2}$ by solution strengthening. The data of zircaloy locate in the lowest stress region among the three because of its weakest solution strengthening. The stress exponent of zircaloy is 4, which is similar to those of h.c.p. metals, though those of AZ31 and Ti-64 are 10 and 30, respectively. It seems that we are observing the power law breakdown similar to that of the highest stress region of CP–Ti. Unfortunately, we cannot discuss further until we perform the precise experiments at lower stresses.

Cubic alloys show negligible creep strain accumulation. Cubic metals show small amount of creep strain accumulation, but only for 1050Al, the minimum creep rate can be estimated as a very low value of 3×10^{-9} s^{-1}. We should not perform the detailed quantitative comparison among the three since the ambient temperature corresponds to 0.32 of the melting point in Kelvin for Al while 0.15 and 0.17 for Ti and Fe, respectively.

4.2 Effect of pre-deformation

Figure 8 shows the creep curves of the cold-rolled CP–Ti and Ti-64. In the annealed state, significant creep strain was observed. In contrast, cold-rolled materials with high dislocation densities demonstrated very slow creep.

4.3 Creep mechanism

Materials with h.c.p. structure show significant creep at an ambient temperature. Among h.c.p. materials, Ti metal and alloy show more extended creep than other h.c.p. materials such as Mg and Zr. The differences among Mg and Zr and among metals and alloys were negligible. The presence of the ambient-temperature creep is summarized in Table 2 in addition to the creep parameters n and $\dot{\varepsilon}_{s0.2}$. The presence of the creep is estimated as ◎ for Ti-64 which has $\dot{\varepsilon}_{s0.2} > 10^{-6}$ s^{-1}, and ○ for the other h.c.p. metals and alloys which

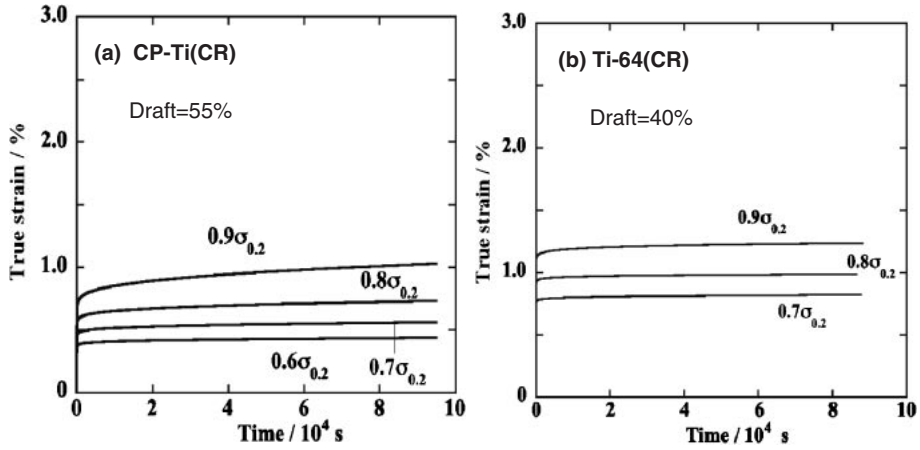

Fig. 8 Creep curves of cold-rolled CP–Ti and Ti-64.

Table 2 Summary of the obtained creep parameters and the evaluation of ambient-temperature creep of the tested metals and alloys.

	Hexagonal (h.c.p.)					cubic				
	c/a (primary slip system)	material	creep parameter		evaluation	structure	material	creep parameter		evaluation
			n	$\dot{\varepsilon}_{s0.2}/10^{-8}\,s^{-1}$				n	$\dot{\varepsilon}_{s0.2}/10^{-8}\,s^{-1}$	
metal	1.59 (prismatic)	CP–Ti	4.1	4.6	○	b.c.c.	pure Fe	—	—	×
		pure Zr	3.0	0.13	○					
	1.62 (basal)	pure Mg	4.7	10	○	f.c.c.	1050Al	0.086	11	○
alloy	1.59 (prismatic)	Ti-64	30	180	◎	f.c.c.	Ti-15333	—	—	×
		Zircaloy	10	0.62	○					
	1.62 (basal)	AZ31	4.3	0.21	○	f.c.c.	5052Al	—	—	×

◎: $\dot{\varepsilon}_{s0.2} > 10^{-6}\,s^{-1}$, ○: $10^{-6}\,s^{-1} > \dot{\varepsilon}_{s0.2} > 10^{-9}\,s^{-1}$, ×: nil strain rate

have $10^{-6}\,s^{-1} > \dot{\varepsilon}_{s0.2} > 10^{-9}\,s^{-1}$. CP–Ti is estimated from the behavior in the lower stress region.

It is obvious that the ambient-temperature creep occurs only in h.c.p. structures. Creep deformation occurs mainly by dislocation creep through dislocation movement, or diffusional creep through atomic diffusion. The ambient-temperature creep can be considered to result of dislocation activity because 1) it occurs at low temperature where no diffusion can take place, 2) stress exponent has a value from 3 to 5, and 3) it is restricted by the pre-deformation as described in the following.

Cold-rolled CP–Ti and Ti-64 with high dislocation densities demonstrated very slow creep. It means that increasing dislocation density by cold-rolling decreases the creep strain rate remarkably. It might be because in the cold-rolled specimen with some amount of dislocation, the peculiar array of dislocations necessary for ambient-temperature creep cannot be introduced.

Further studies are necessary to reveal the dislocation activity during the ambient-temperature creep and why time dependent deformation can be possible at an ambient temperature where no diffusion can take place.

5. Conclusions

Tensile and creep tests were performed using typical annealed h.c.p., f.c.c. and b.c.c. metals and alloys at an ambient temperature. While cubic metals and alloys demonstrated negligible creep in all stress ranges, h.c.p. metals and alloys demonstrated significant creep. Among h.c.p. materials, Ti metals and alloys show more extended creep than other h.c.p. materials such as Mg and Zr metals and alloys. The difference among Mg and Zr metals and alloys were negligible. This ambient-temperature creep was largely slowed down by pre-deformation.

Acknowledgement

Part of this study was supported by the Light Metal Educational Foundation, Inc.

REFERENCES

1) A. W. Thompson and B. C. Odegard: Metall. Trans. A **4** (1973) 899–908.
2) B. C. Odegard and A. W. Thompson: Metall. Trans. A **5** (1974) 1207–1213.
3) M. A. Imam and C. M. Gilmore: Metall. Trans. A **10** (1979) 419–425.
4) W. H. Miller, R. T. Chen and E. A. Starke: Metall. Trans. **18A** (1987) 1451–1467.
5) S. Ankem, C. A. Greene and S. Singh: Scr. Metall. **30** (1994) 803–808.
6) S. Suri, G. B. Viswanathan, T. Neeraji, D. H. Hou and M. J. Mills: Acta Mater. **47** (1999) 1019–1042.
7) T. Neeraj, D. H. Hou, G. S. Daehn and M. J. Mills: Acta Mater. **48** (2000) 1225–1238.
8) T. Neeraj and M. J. Mills: Mater. Sci. Eng. A **319–321** (2001) 415–419.
9) V. Hasija, S. Ghosh, M. J. Mills and D. S. Joseph: Acta Mater. **51** (2003) 4533–4549.
10) A. H. Cottrell: Philos. Mag. **74** (1996) 1041–1046.
11) T. Yamada, K. Kawabata, E. Sato, K. Kuribayashi and I. Jimbo: Mater. Sci. Eng. A **387–389** (2004) 719–722.